Proceedings of the 3rd International Conference on Mechatronics and Smart Systems
DOI: 10.54254/2755-2721/141/2025.22047

Structural Design and Optimization of Aerial Robots for Tree Barrier Clearing Operations

Yuanwei Dai

School of Mechanical Engineering, Northwestern Polytechnical University, Xi'an, China
dyw050509@mail.nwpu.edu.cn

Abstract: This paper focuses on the structural design of an aerial robot applied to tree barrier clearing operations. First, the robot's structure is abstractly divided into three main components: the ventral propulsion system, the X-configuration quadrotor fuselage, and the operational robotic arm. The roles and mechanical characteristics of each component during operation are analyzed in detail. By introducing relevant mechanical formulas, the calculation and optimization methods for propulsion thrust, rotor control torque, and robotic arm cutting forces are thoroughly explored. Based on this, design improvement schemes such as material optimization, ventral propulsion system optimization, structural optimization, and dual-mode optimization (no-load and operational modes) are proposed to enhance the robot's flight performance, operational flexibility, and energy efficiency.

Keywords: Aerial robot, Dynamic modeling, Ventral propulsion system, Variable-pitch propeller, Tilting joint

1. Introduction

In recent years, operational aerial robots have garnered significant attention, demonstrating immense potential in fields such as forestry management, power line inspection, and agricultural protection. Compared to traditional tree barrier clearing methods, aerial robots offer distinct advantages: First, they can replace humans in hazardous environments, greatly ensuring personnel safety. Second, they can efficiently perform repetitive tasks, saving labor and time costs. Additionally, aerial robots can adapt to complex terrains, completing high-altitude tasks that are difficult for humans to reach. However, despite their many advantages in practical applications, operational aerial robots still face several technical difficulties, such as short endurance, limited flexibility, and poor stability in complex environments. These issues hinder the further adoption of aerial robots in tree barrier clearing operations.

Compared to existing methods, operational aerial robots still face numerous challenges in structural design and performance optimization. To deal with shortage in aerial robots, [1-3] primarily introduced the structural modeling and control methods of quadrotor drones, proposing state estimation-based control algorithms and open-loop control-based rapid maneuvering methods to achieve quick attitude adjustments, significantly improving flight stability. However, these studies do not address the application of drones in aerial operations or the integration of robotic arms. For drones' specific application issue, a lightweight robotic arm design and control methods were proposed by [4-6], significantly enhancing the arm's load capacity and durability. Additionally, [7-8] introduced force feedback-based control strategies and cooperative control methods between the robotic arm and

© 2025 The Authors. This is an open access article distributed under the terms of the Creative Commons Attribution License 4.0 (https://creativecommons.org/licenses/by/4.0/).

DOI: 10.54254/2755-2721/141/2025.22047

the flight platform, significantly improving operational precision and efficiency. However, these studies do not resolve the flight stability issues during robotic arm operations. To solve this problem, a quadrotor system equipped with a two-degree-of-freedom robotic arm was designed in [9], demonstrating the drone's adaptability to robotic arm movements and external disturbances while maintaining flight stability. However, the limited degrees of freedom of the robotic arm restrict its flexibility and operational range in complex tasks. In summary, although existing research has made progress in certain areas, operational aerial robots still face significant shortcomings in flight stability in complex environments, dynamic load optimization during robotic arm operations, real-time efficiency of propulsion thrust allocation, and endurance. Addressing these issues requires comprehensive optimization in structural design, material selection, and control algorithms.

This paper addresses the above problems by proposing a new structural design for operational aerial robots and systematically optimizing them. The main contributions of this paper include: (1) A mechanical model of the aerial robot has been proposed, providing a theoretical basis for structural design; (2) Material optimization, ventral propulsion system optimization, structural optimization, and dual-mode optimization have been designed, significantly improving the robot's endurance, operational flexibility, and environmental adaptability; (3) Variable-pitch propellers and tilting joint designs have been introduced to address previously unresolved issues of high-speed flight stability and adaptability to complex environments, offering a more reliable technical pathway for the practical application of operational aerial robots.

2. Structural Design of Operational Aerial Robots

This section focuses on the structural design of aerial robots for tree barrier clearing operations. First, the robot's structure is abstractly divided into three main components, and the roles and impacts of each component during operation are explained in detail, incorporating relevant mechanical formulas for deeper analysis.

2.1. Overall Structure Overview

During tree barrier clearing operations, the aerial robot carries an operational robotic arm at the center of its ventral axis and is equipped with a propulsion system in the ventral position. This layout provides critical hardware support for the robot's operations. The overall structure is shown in Figure 1. The meanings of some symbols used in this paper are listed in Table 1.

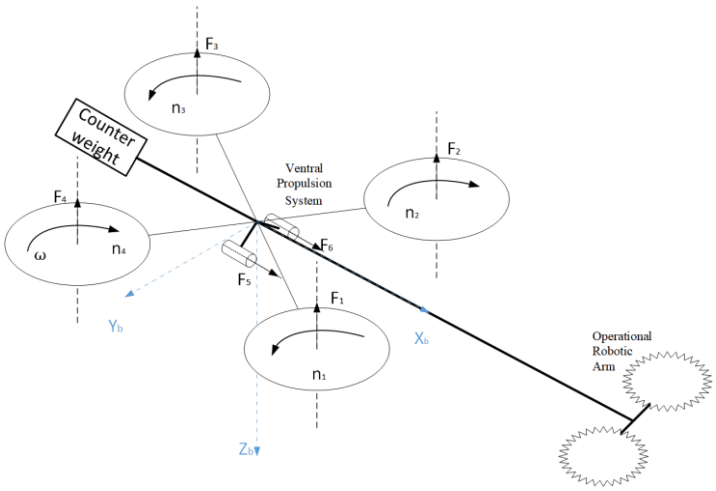

Figure 1: Schematic diagram of the operational aerial robot model.

DOI: 10.54254/2755-2721/141/2025.22047

Table 1: Meanings of commonly used symbols in this paper.

Symbol	Meaning
γ	Body position
ω	Body rotation speed
$n_1 \sim n_4$	Rotor speeds of the quadrotor
$F_1 \sim F_4$	Thrust generated by each rotor
M_r	Three-axis resultant torque of the quadrotor system
$n_5 \sim n_6$	Speed of the ventral propulsion system
$F_5 \sim F_6$	Thrust generated by the ventral propulsion system
M_t	Three-axis torque generated by the propulsion system
$F_7 \sim F_8$	Cutting force generated by the operational tool

2.2. Structural Components

2.2.1. Ventral Propulsion System

Two propulsion units are symmetrically suspended below the ventral section, distributed on either side. The input parameter for the propulsion system is the desired motor speed, and the output are thrust and torque. The relationship is as follows:

$$F_5 = k_{tf} n_5^2, F_6 = k_{tf} n_6^2 \tag{1}$$

where k_{tf} is the thrust coefficient of the propulsion system.

By adjusting the motor speed, the thrust F can be precisely controlled. The three-axis torque M_t generated by the propulsion system mainly consists of the torque caused by thrust not passing through the center of mass and the motor's reaction torque, expressed as:

$$M_t = \begin{pmatrix} 0 \\ l_{ty} \\ l_{tz} \end{pmatrix} \times \begin{pmatrix} f_5 \\ 0 \\ 0 \end{pmatrix} + \begin{pmatrix} 0 \\ -l_{ty} \\ l_{t=} \end{pmatrix} \times \begin{pmatrix} f_6 \\ 0 \\ 0 \end{pmatrix} + k_{tm} \begin{pmatrix} n_6^2 - n_5^2 \\ 0 \\ 0 \end{pmatrix} \tag{2}$$

where l_{ty} and l_{tz} are the projected lengths of the distances between the centers of mass of the two symmetrically distributed propulsion units and the center of mass of the aircraft on the y_b and z_b axes, respectively, and k_{tm} is the reaction torque coefficient of the propulsion system.

During low-speed flight of the unmanned helicopter, the condition $M_t = 0$ must be satisfied. Under this condition, the two propulsion systems can effectively counteract the reaction torque, preventing the fuselage from rotating. In high-speed flight, the thrust generated by the propulsion systems helps increase the flight speed of the unmanned helicopter. According to Newton's second law ($F = ma$, where F is the net force, m is the mass of the drone, and a is the acceleration), the additional thrust provided by the propulsion systems enables the drone to achieve greater acceleration, thereby enhancing its flight speed.

2.2.2. X-Configuration Quadrotor fuselage

This component is analogous to a standard X-configuration quadrotor drone, providing the robot with basic flight capabilities to ensure stable flight and task execution. The quadrotor adjusts its flight attitude and direction by controlling the speeds of its four rotors. The thrust F generated by each rotor is parallel to the negative z_b axis and related to the rotor speed n as follows:

DOI: 10.54254/2755-2721/141/2025.22047

$$F_i = k_{rf} n_i^2, i = 1,2,3,4 \tag{3}$$

where k_{rf} is the rotor lift coefficient.

Considering reaction torque, the three-axis resultant torque of the quadrotor system is related to the rotor speeds as follows:

$$M_r = \begin{pmatrix} -l_r k_{tf} & l_r k_{tf} & l_r k_{tf} & -l_r k_{tf} \\ l_r k_{rf} & l_r k_{rf} & -l_r k_{rf} & -l_r k_{rf} \\ -k_{rm} & k_{rm} & -k_{rm} & k_{rm} \end{pmatrix} \begin{pmatrix} n_1^2 \\ n_2^2 \\ n_3^2 \\ n_4^2 \end{pmatrix} \tag{4}$$

where l_r is the projection length of the distance between each rotor and the center of mass on the x_b or y_b axis (also known as the moment arm), and k_{rm} is the reaction torque coefficient.

2.2.3. Operational Robotic Arm

During operations, the robotic arm equipped with a cutting tool needs to move away from the target. The cutting forces F_7, F_8 are decomposed into a main cutting force F_x and a reaction force F_y from the tree branch. Since the reaction force F_y passes through the robot's center of mass, it does not affect the attitude channel. Therefore, only the disturbance caused by the main cutting force F_x is considered. The disturbance torque $bm\tau_c$ generated by the main cutting force is as follows:

$$\tau_c = F_x l_s b_3 \tag{5}$$

where $b_3 = [0\ 0\ 1]^T$ and l_s is the distance from the cutting tool's tip to the robot's center of mass. The main cutting force F_x can be calculated as:

$$F_x = \frac{KV_0}{v} = \frac{P_c}{v} \tag{6}$$

where V_0 represents the volume of branches cut by the saw blade per unit time, P_c is the cutting power, K is energy required to cut a unit volume of branch and v is the cutting speed. Additionally,

$$P_e = P_c + P_0 \tag{7}$$

where P_0 and P_e represent the no-load power and electromagnetic power of the DC motor, respectively.

2.3. Optimization Design

2.3.1. Material Optimization

New materials with high strength and lightweight properties are selected to reduce the robot's overall weight while ensuring structural strength. This reduces energy consumption, improves energy efficiency, and extends the robot's endurance.

2.3.2. Ventral Propulsion System Optimization

A variable-pitch propeller with precisely controllable blade angles is designed. The thrust is related to factors such as pitch and speed, generally satisfying:

$$F = C_p \bullet \rho \bullet n^2 \bullet D^4 \tag{8}$$

where C_p is the thrust coefficient, related to pitch and other factors. By adjusting the pitch, the thrust coefficient C_p can be changed, thereby adjusting the thrust. Aerodynamic simulation technology is

DOI: 10.54254/2755-2721/141/2025.22047

used to optimize the propeller's shape, enabling automatic pitch adjustment in different flight states to achieve optimal thrust and improve flight performance and operational efficiency.

2.3.3. Structural Optimization

To address the limitations of fixed-angle tools in complex environments, a tilting joint is added between the rigid frame and the tool system. This joint, equipped with a motor, allows the tool system to perform pitch movements and lock at specific angles. In addition, a tilting joint is added between the propulsion system and the frame, enhancing the robot's flexibility and adaptability during operations.

2.3.4. Dual-Mode Optimization (No-Load and Operational Modes)

A detachable hook mechanism is installed between the suspension system and the flight platform, allowing the robot to switch between no-load and operational modes based on task requirements. This improves operational efficiency and user convenience. During the mode switching, the system's stability and dynamic characteristics should be considered to ensure balanced forces and avoid affecting flight stability.

3. Conclusion

This paper has investigated the requirements of tree barrier clearing operations by designing and optimizing a dedicated aerial robot structure. First of all, a mechanical model of the aerial robot has been proposed to establish a theoretical basis for structural design. Then, variable-pitch propellers, tilting joints and dual-mode have been designed, which significantly improves the robot's endurance and operational efficiency. Through continuous optimization and innovation, the research results of this paper will provide stronger technical support for the application of aerial robots in tree barrier clearing operations. Future work will focus on studying multi-robot cooperative control strategies.

References

[1] *Mahony, R., Kumar, V., & Corke, P. (2012). Multirotor aerial vehicles: Modeling, estimation, and control of quadrotor. IEEE Robotics & Automation Magazine, 19(3), 20-32.*
[2] *Beard, R. W., & McLain, T. W. (2012). Small unmanned aircraft: Theory and practice. Princeton University Press.*
[3] *Lupashin, S., & D'Andrea, R. (2014). Adaptive fast open-loop maneuvers for quadrocopters. Autonomous Robots, 36(1-2), 123-142.*
[4] *Kondak, K., Bernard, M., & Hommel, G. (2015). Design and control of a lightweight aerial manipulator. In 2015 IEEE International Conference on Robotics and Automation (ICRA)(pp. 4693-4698). IEEE.*
[5] *Ruggiero, F., Lippiello, V., & Ollero, A. (2018). Aerial manipulation: A literature review. IEEE Robotics & Automation Letters, 3(3), 1957-1964.*
[6] *Oh, P., Jang, K., & Kim, D. (2017). Design and control of a lightweight aerial manipulator for outdoor applications. International Journal of Advanced Robotic Systems, 14(5), 1-12.*
[7] *Ollero, A., & Heredia, G. (2016). Stability analysis of an aerial manipulator for contact-based inspection. IEEE Transactions on Robotics, 32(4), 799-806.*
[8] *Orsag, M., Korpela, C., & Oh, P. (2014). Modeling and control of an aerial manipulator for contact-based inspection. Journal of Intelligent & Robotic Systems, 73(1-4), 469-483.*
[9] *Orsag, M., Korpela, C., & Oh, P. (2021). Aerial manipulation using a quadrotor with a two-degree-of-freedom robotic arm. Journal of Intelligent & Robotic Systems, 102(3), 1-15.*